INORGANIC CHEMISTRY FRONTIERS

RESEARCH ARTICLE

View Article Online
View Journal | View Issue

Cite this: *Inorg. Chem. Front.*, 2022, **9**, 6596

The rare-earth derivant of mixed-polyoxoniobate clusters with high proton release capacity†

Haiying Wang,‡[a] Xiaohan Xu,‡[b] Qianqian Shang,[a] Kexing Xiao,[b] Jiahui Chen,[b] Yuqing Yang,[b] Ehsan Raee,[b] Dongdi Zhang, *[a] Jingyang Niu *[a] and Tianbo Liu *[b]

A family of rare-earth derivant mixed-polyoxoniobate clusters $K_{12}(NH_4)_{10}[\{Nb_{12}P_4W_{24}O_{122}\}_2\{Ln(H_2O)_5\}_4\{Nb_4O_4(OH)_6\}]\cdot xH_2O$ (Ln = Sm, Eu, Tb, Dy, Er, Tm and Yb for **1–7**, abbreviated as $\{Ln_4Nb_{28}\}$) were synthesized and structurally characterized by single-crystal X-ray diffraction, elemental analyses, IR spectroscopy and TG analyses. Containing four Wells–Dawson $[Nb_6P_2W_{12}O_{62}]^{12-}$, a $\{Nb_4O_6\}$ core, and four Ln^{III} ions, the polyanions in **1–7** are a group of rare-earth derivants of phosphoniobotungstates. These water-soluble clusters behave as weak acids with good stability and high proton release capacity depending on the pH. Each cluster carries ~22 negative charges in the aqueous solution without any deprotonation with the pH the same as that used for deionized water. Upon the introduction of bases, they get deprotonated gradually and each anion cluster can release up to 20 protons from its 20 coordinated water ligands. The pK_a values of these acidic clusters with different degrees of deprotonation range from ~8.3 to ~10.5. Moreover, these clusters demonstrate an increasing deprotonation efficiency with the decreasing ionic radius of incorporated Ln^{III} ions, which could be attributed to the lanthanide contraction. In other words, the $\{Ln_4Nb_{28}\}$ macroanion clusters with smaller Ln^{III} centers are easier to deprotonate due to their shorter and stronger Ln–O bonds. This is the first study that focuses on the effect of lanthanide contraction on proton release in polyoxometalate chemistry. The $\{Ln_4Nb_{28}\}$ clusters with good stability, high proton release capacity, and controllable deprotonation efficiency provide models for the understanding of protonated polyelectrolyte solutions, and the design and applications of polyoxometalate-based protonated materials.

Received 12th September 2022,
Accepted 30th October 2022

DOI: 10.1039/d2qi01953a

rsc.li/frontiers-inorganic

Introduction

Polyoxometalates (POMs), a family of molecular clusters composed of metal oxide polyhedra as building blocks, have been applied broadly in catalysis, photo-electronic/magnetic materials, POMs/polymer composite materials, and biologically active materials.[1,2] Many types of POM clusters are macroanions in the aqueous solution, while some others are neutral or macrocations. It is particularly interesting that besides the inherent charges on the clusters, they can sometimes experience additional protonation or deprotonation in the aqueous solution, with their coordinated water ligands being a major source. Such clusters can behave like weak Brønsted acids, which affects their solution behaviors including solubility, oxidation and reduction, and their consequent self-assembly into "blackberry"-type structures. For instance, we systematically investigated the pH-dependent deprotonations of a series of Keplerate-clusters including $\{Mo_{72}V_{30}\}$, $\{Mo_{72}Cr_{30}\}$ and $\{Mo_{72}Fe_{30}\}$, and their self-assembly processes in solution.[3,4] In addition, the catalytic activities of some POM clusters could be triggered by and rely on the deprotonation/protonation of their aqua and/or hydroxyl ligands, due to the effect of deprotonation/protonation on the surrounding coordination bonds.[5,6]

Moreover, with deprotonation/protonation as one of the most widely applied and fundamental stimuli, the clusters can be used as model systems to help understand and design the deprotonation/protonation of functional stimuli-responsive materials, such as protonated polymers and proteins,[7–9] and the molecular hybrid of POMs and metal nanoclusters.[10]

Some POM molecular clusters with coordinated water ligands can reversibly release protons from their water ligands into the aqueous solution. They can therefore be treated as

[a]*Henan Key Laboratory of Polyoxometalate Chemistry, College of Chemistry and Chemical Engineering, Henan University, Kaifeng 475004, P. R. China. E-mail: ddzhang@henu.edu.cn, jyniu@henu.edu.cn*

[b]*School of Polymer Science and Polymer Engineering, The University of Akron, Akron, Ohio 44325, USA. E-mail: tliu@uakron.edu*

†Electronic supplementary information (ESI) available. CCDC 2194738–2194744. For ESI and crystallographic data in CIF or other electronic format see DOI: https://doi.org/10.1039/d2qi01953a

‡These authors contributed equally to this work.

weak acids with multiple deprotonation sites. Such a deprotonation process is usually pH dependent, as a feature of weak acids.[3,4,6,11,12] In some cases, with a large number of water ligands, the deprotonation capacity could be rather high. For example, a molecular cluster with the formula of $K_{41}[(P_2W_{12}Nb_6O_{62})_6\{Mn_3(OH)_3(H_2O)_6\}_4\{Mn_3Na(H_2O)_{16}\}]\cdot 26H_2O$, is an extremely weak acid with a high proton release capacity of up to 40 protons.[11] Moreover, the deprotonation potential relates to the geometry of the acidic sites. For some Keplerate-type clusters, the water ligands staying on the external surface of the cluster demonstrate pH-dependent deprotonation, while those ligands inside the Keplerate capsules could not release free protons into the solution because protons could not pass through the negatively charged surface pores on the surface of clusters.[3] Another type of deprotonation is enabled by the cavity of clusters that can accommodate a few protons *via* hydrogen bonds.[13]

Herein, a family of rare-earth derivant mixed-polyoxoniobate clusters has been presented as a tetramer with a general formula of $K_{12}(NH_4)_{10}[\{Nb_{12}P_4W_{24}O_{122}\}_2\{Ln(H_2O)_5\}_4\{Nb_4O_4(OH)_6\}]\cdot xH_2O$ (Ln = Sm x = 85, Eu x = 65, Tb x = 85, Dy x = 85, Er x = 85, Tm x = 85, Yb x = 85 for **1–7**, abbreviated as $\{Ln_4Nb_{28}\}$), and a dimension of 2.3 × 2.0 × 2.0 nm^3 (Fig. 1). As far as we know, they are the rare examples of rare-earth derivatives of phosphoniobotungstates. It would be interesting to examine if such clusters can deprotonate their coordinated water ligands, and if they can, whether such processes are pH dependent as speculated. Moreover, this series of samples provide a valuable opportunity to compare the effect of lanthanide ions incorporated into the clusters – they are expected to demonstrate very similar chemical features; a noticeable difference among them would be their ionic sizes due to the so-called lanthanide contraction effect – leading to smaller ionic size for heavier Ln-series elements.

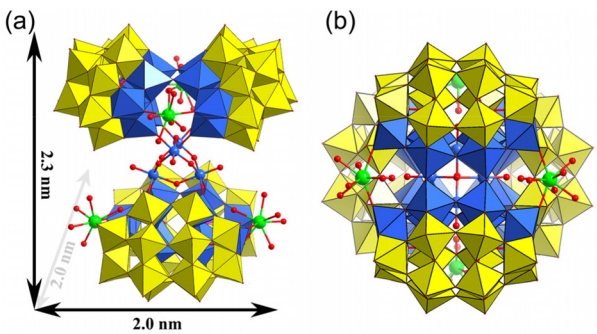

Fig. 1 (a, b) Polyhedral and ball-and-stick representation of the isostructural $\{Ln_4Nb_{28}\}$ polyanions from different directions. Color codes: W, yellow; Nb, blue; P, purple; Ln, green; O, red; WO_6 polyhedral, yellow; and NbO_6 polyhedral, blue.

Results and discussion

Structure characterization

Single-crystal X-ray diffraction analysis (Table S1†) reveals that the polyanion $\{Ln_4Nb_{28}\}$ crystallizes in the orthorhombic system *Fddd* space-group. The polyanion in **1–7** is a rare-earth derivant tetramer based on mixed-addendum niobotungstate containing four Wells–Dawson $[Nb_6P_2W_{12}O_{62}]^{12-}$ ($Nb_6P_2W_{12}$), a $\{Nb_4O_6\}$ core, four Ln^{3+} ions, 12 K^+, 10 NH_4^+ and crystal molecules. The six lacunary sites of $[P_2W_{12}O_{48}]^{14-}$ are occupied by six $\{NbO_6\}$ octahedra forming the saturated mixed-Wells–Dawson $\{Nb_6P_2W_{12}\}$ unit (Fig. S1†). Two $[Nb_6P_2W_{12}O_{62}]^{12-}$ units are linked together by equatorial Nb–O–Nb bridges forming a $\{Nb_{12}P_4W_{24}O_{122}\}$ dimer (Fig. 2a). The terminal oxygens (O_t) of $\{NbO_6\}$ octahedra have higher nucleophilicity relative to $\{WO_6\}$ octahedra because of the uneven charge density distribution which is caused by the different oxidation states of W^{6+} and Nb^{5+}, resulting in the easier coordination ability with Ln^{3+} ions. Two Ln^{3+} ions are located at both ends of the dimer and are connected to the polar $\{NbO_6\}$ octahedron by Nb–O–Ln bridges (Fig. 2b and c). The Ln^{3+} derived dimers face each other, crisscross, and are connected by a central $\{Nb_4O_6\}$ core (Fig. 2d) *via* eight Nb–O–Nb bridges, and

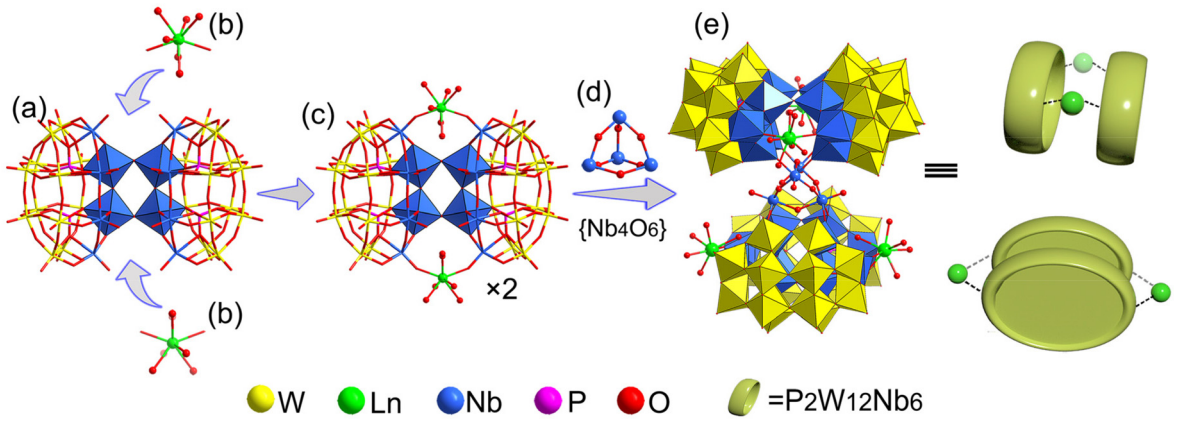

Fig. 2 (a) Polyhedral and ball-and-stick representations of the $\{Nb_{12}P_4W_{24}O_{122}\}$ dimer; (b) the Ln^{3+} ions; (c) the Ln^{3+} derived dimer composed of Ln^{3+} and $\{Nb_{12}P_4W_{24}O_{122}\}$; (d) the $\{Nb_4O_6\}$ core; (e) the polyanion in compounds **1–7**.

finally forming the tetrameric structure of the polyanion (Fig. 2e). Actually, the polyanion can also be viewed as a Ln^{3+} ion derivant of the structure we reported in 2014.[14] To our knowledge, this is a rare report about the example of a rare-earth derivant based on niobotungstate chemistry.[15] In addition, the polyanion can be extended into a purely inorganic three-dimensional metal frame if the peripheral K^+ cations act as linkers (Fig. S2†). All of the Nb atoms in the polyanion show hexa-coordinate octahedron configuration. For the Ln^{3+} ions, all of them are coordinated with two bridge oxygen (μ_2-O) and six terminal aqua ligands resulting in the eight-coordinate two-capped triangular prism geometry (Fig. S3†). However, crystallographic refinement indicates that the occupancy factors of O5 W and O6 W are both 0.5, leading to $[Ln(H_2O)_5]^{3+}$. The Ln–O bond lengths are reduced, which are generally in agreement with the ion radius trend in the lanthanide elements (Table S2†).

Bond valence sum (BVS) calculations[14] are carried out on all the Ln, Nb, P and W centers (Table S3†) and the results show the 3+, 5+, 5+ and 6+ oxidation states, respectively. The BVS values of all the O oxygen atoms indicate that the μ_2-O of O64 and O65 are monoprotonated with values in the range of 0.79–1.44 resulting in the $\{Nb_4O_4(OH)_6\}$ core. It should be noted that the molecular formula was finally determined according to the crystal analysis, charge balance, ICP-OES, CHN elemental analysis and TGA.

Deprotonation in aqueous solution

Each $\{Ln_4Nb_{28}\}$ cluster carries ~22 negative charges with 12 K^+ and 10 NH_4^+ counterions. When dissolved in water, they release all their counterions into the solution (Table S4†). The pH of these solutions (at 1.0 mg mL^{-1}) is ~5.70, suggesting that there is no protonation/deprotonation from the clusters in pure water. This is further confirmed by conductivity measurements (Table S4†). When KOH was gradually introduced into the solutions of the clusters, the pH increment during this titration was slower than introducing the same amount of KOH into pure water. For example, the pH of 1.0 mg mL^{-1} $\{Sm_4Nb_{28}\}$ solution containing 10 equiv. of KOH (molar ratio of KOH/clusters = 10) is 8.39; while the same amount of KOH in pure water leads to a pH of 10.73 (Fig. 3). This indicates that some protons are released from the clusters to neutralize the OH^-, *i.e.*, the clusters act as weak acids with a buffering effect by showing a pH-dependent proton release feature.

The number of protons released per cluster can be calculated by the pH difference between the aqueous solution of the clusters and pure water (reference) when the same amount of KOH is added. The solution preparation and pH measurements were conducted under a N_2 atmosphere (in a glovebox). The deionized water used in experiments was boiled in advance to avoid CO_2 dissolution neutralizing KOH. The deprotonation process of the $\{Sm_4Nb_{28}\}$ cluster is given in Fig. 4 as an example. With the introduction of up to 30 equiv. of KOH, the titration curve shows that the majority of hydroxide introduced is neutralized quickly and linearly. In this stage (0–30 equiv. of KOH), there is a linear relationship between the amount of KOH introduced and the number of deprotonations from each cluster with a slope of 0.73. With the further addition of KOH, 40 equiv. of KOH leads to the final deprotonation of ~30 ± 3 protons, and the clusters do not further release any protons even with excess KOH. All solutions do not display any colour change or precipitation during the experiments for up to one year, which suggests the good stability of these acidic clusters in highly basic environments. Besides, the polyanions can remain intact throughout the titration experiment, as demonstrated by negative-ion ESI mass spectra (Fig. S5–S7, Table S13†). It is noted that the deprotonation process of clusters during the period of addition of 30–40 equiv. of KOH is not a linear growth anymore, showing that it is more difficult for the highly negatively charged clusters to release protons. Nevertheless, not all of the 30 released protons stem from the anion cluster. As shown in Fig. 5, the hydrolysis of NH_4^+ ions would be expected to occur in a basic solution. The degree of hydrolysis can be determined by the difference in pH between the aqueous solution of NH_4Cl containing KOH (with a concentration of NH_4^+ the same as that in

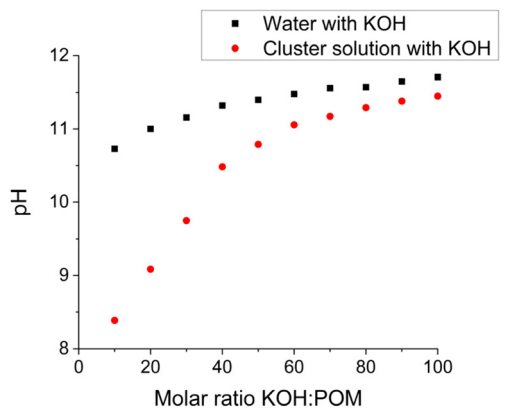

Fig. 3 The pH response of introducing KOH into pure water and 1.0 mg mL^{-1} $\{Sm_4Nb_{28}\}$ cluster solution.

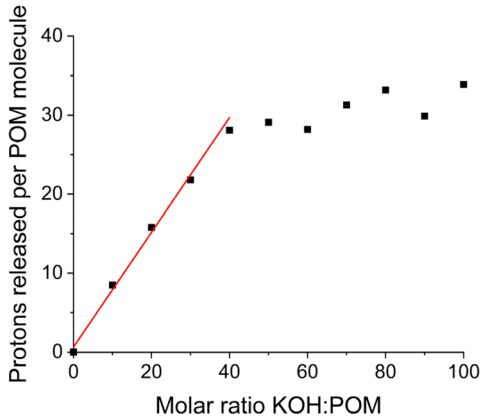

Fig. 4 The number of protons released per molecular cluster (including the protons contributed by the hydrolysis of ammonium ions) *versus* the molar ratio of KOH introduced to $\{Sm_4Nb_{28}\}$ clusters.

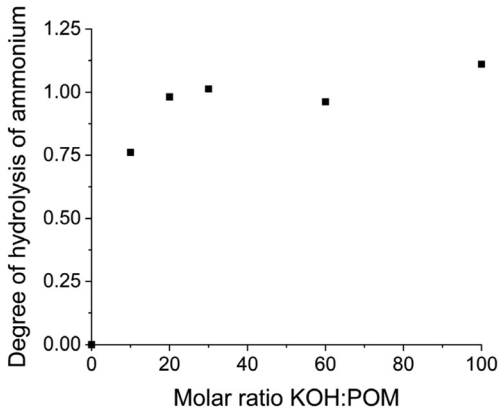

Fig. 5 The degree of hydrolysis of ammonium *versus* the molar ratio of KOH introduced to POM clusters. The degree of hydrolysis can be calculated by the difference in pH between the aqueous solution of NH_4Cl containing KOH (with a concentration of NH_4^+ the same as that in $\{Ln_4Nb_{28}\}$ solution) and water containing the same amount of KOH. The molar ratio of KOH and POM is used as the abscissa for convenience to compare the hydrolysis process and the deprotonation process.

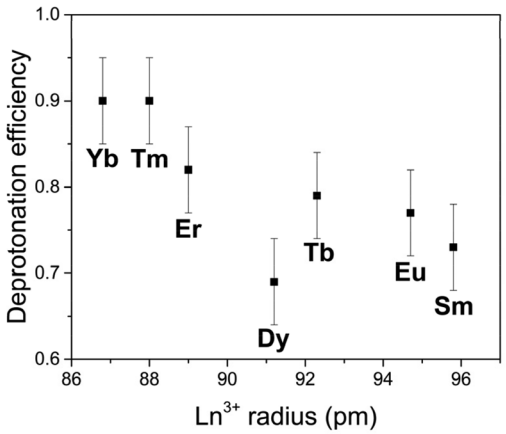

Fig. 6 Deprotonation efficiency of $\{Ln_4Nb_{28}\}$ clusters *versus* the ionic radii of Ln^{III} centers. The deprotonation efficiency, which is calculated by the ratio of the number of protons released per entire POM molecule over the molar ratio of KOH/cluster, indicates the number of protons released per entire POM molecule with the introduction of 1 equiv. of KOH.

$\{Ln_4Nb_{28}\}$ solution) and water containing the same amount of KOH. Assuming that the NH_4^+ ions experience the same extent of hydrolysis in the NH_4Cl solution and the cluster solutions, the number of protons released from the anion in the $\{Sm_4Nb_{28}\}$ cluster can be calculated by subtracting the contribution of NH_4^+, as shown in Table S5.† Consequently, 10 of the 30 protons are attributed to the hydrolysis of NH_4^+ ions, indicating that each anion cluster can release up to ~20 protons eventually.

All members of this family of rare-earth clusters demonstrate a similar deprotonation behaviour: they release protons linearly in an early stage with up to 30 equiv. of KOH added and stop deprotonating after releasing ~20 protons from the original anion with the introduction of ~40 equiv. of KOH (Fig. S4†). These 20 protons released easily from the macroanion suggest the most possible deprotonation sites, *i.e.*, the 20 coordinated water ligands on the cluster.

The deprotonation capacity of these rare-earth derivant clusters was qualitatively explored by comparing their deprotonation efficiency in the linear stage of deprotonation (with the addition of 0–30 equiv. of KOH). The deprotonation efficiency is calculated by the ratio of the number of protons released per entire POM molecule (from both the anionic cluster and the ammonium ions) over the molar ratio of KOH/cluster, *i.e.*, the slope of the linear part in Fig. 4. The deprotonation efficiency suggests the number of protons that an entire cluster can provide with the introduction of 1 equiv. of KOH. As shown in Fig. 6, with the decreasing ionic radius of the Ln^{III} center in the cluster, the deprotonation efficiency increases monotonically from 0.73 (Sm) to 0.90 (Yb). In other words, a smaller Ln^{III} center leads to a higher deprotonation efficiency. We attribute this observation to the continuously increasing charge density, *i.e.*, Lewis acidity, of Ln^{III} in the coordination complex $[Ln^{III}(H_2O)_5]^{3+}$ due to the well-known lanthanide contraction.[16] A higher charge density of Ln^{III} leads to stronger coordination between Ln^{III} and O, making the protons linked to the oxygen atoms easier to be released from the cluster. This trend of deprotonation efficiency is consistent with our observation that the Ln–O bond length decreases with the decreasing ionic radius of Ln^{III} (Table S2†). It also agrees with some earlier reports that smaller Ln^{III} results in a shorter Ln–O bond length in POM clusters.[17,18]

The deprotonation processes of the $\{Ln_4Nb_{28}\}$ clusters are quite different from typical polyprotic acids which have multiple distinguishable titration stages that may overlap with each other. The linearly increasing pH during the titration shown in Fig. 3 suggests the small and continuous increment in the successive acid dissociation constant (pK_a) of the clusters and the overlap between the pH ranges of the dissociation equilibria of the clusters with different degrees of deprotonation. In other words, the multiple deprotonation sites on each cluster are independent of each other. However, with more and more deprotonations occurring on the same cluster, the departure of future protons becomes slightly more difficult. This deprotonation feature is consistent with our observation of another POM cluster.[11] Overall, it reveals a feature that the cluster's deprotonation behavior can be briefly described by one pK_a value; or to be more accurate, a series of increasing pK_a values corresponding to an increasing amount of the added base. Assuming that the deprotonation of clusters has no impact on the hydrolysis of the NH_4^+, the pK_a values of clusters can be calculated based on the deprotonation efficiency after subtracting the contribution of NH_4^+, as shown in Fig. 7. The clusters with a few deprotonations have acidities slightly higher than NH_4^+ (pK_a of NH_4^+ = 9.25), while the clusters after releasing a number of protons, *e.g.*, ~12 protons with 30 equiv. of KOH, are less acidic than NH_4^+. The cluster solution with 40 equiv. of KOH at pH = 10.5 can be used as an

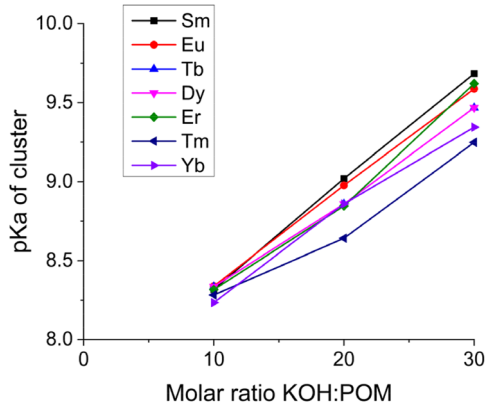

Fig. 7 The pK_a values of the {Ln_4Nb_{28}} clusters during the deprotonation process.

approximation of pK_a of the cluster carrying one acidic proton, because 40 equiv. of KOH is just right for each anion cluster to release ~20 protons and all NH_4^+ ions have already hydrolyzed with ~20 equiv. of KOH. Overall, the pK_a values of these clusters with different deprotonations are in the range of 8.3–10.5 roughly. A sample pK_a calculation is provided in the ESI.†

Conclusions

In summary, the synthesis and structures of the rare examples of rare-earth derivants based on hexalacunary niobotungstate are reported. The polyanions in this new family are rare-earth derivant tetramers based on Nb/W mixed-addendum POM clusters. Depending on the pH, the clusters exhibit a high proton release capacity. Each cluster can deprotonate up to 20 protons from their coordinated water ligands in the basic solution. Moreover, these clusters with different Ln^{III} centers demonstrated an increased deprotonation efficiency with a smaller ionic radius of Ln^{III} due to lanthanide contraction. A smaller Ln^{III} center with a higher charge density forms shorter/stronger coordination bonds with the oxygen in the water molecule, thus making the protons in the coordinated water ligands easier to be released. The pK_a values of these clusters slightly increase from ~8.3 to ~10.5 when more base was added (and consequently more protons were deprotonated), with the clusters having smaller Ln^{III} centers exhibiting pK_a values slightly lower than the others. The understanding of deprotonation features of such POM clusters provides a reference for both fundamental studies and applications of (POM-based) protonated materials.

Conflicts of interest

There are no conflicts to declare.

Acknowledgements

This work was supported by the National Natural Science Foundation of China (21671056 and 22071045), the Excellent Youth Science Fund Project of Henan Province (202300410042) and Henan University. T. L. acknowledges support from the National Science Foundation (CHE2132178) and The University of Akron.

References

1 Y.-F. Song and R. Tsunashima, Recent advances on polyoxometalate-based molecular and composite materials, *Chem. Soc. Rev.*, 2012, **41**, 7384–7648.
2 D.-L. Long, E. Burkholder and L. Cronin, Polyoxometalate clusters, nanostructures and materials: From self assembly to designer materials and devices, *Chem. Soc. Rev.*, 2007, **36**, 105–121.
3 M. L. Kistler, T. Liu, P. Gouzerh, A. M. Todea and A. Müller, Molybdenum-oxide based unique polyprotic nanoacids showing different deprotonations and related assembly processes in solution, *Dalton Trans.*, 2009, **26**, 5094–5100.
4 T. Liu, B. Imber, E. Diemann, G. Liu, K. Cokleski, H. Li, Z. Chen and A. Müller, Deprotonations and Charges of Well-Defined {$Mo_{72}Fe_{30}$} Nanoacids Simply Stepwise Tuned by pH Allow Control/Variation of Related Self-Assembly Processes, *J. Am. Chem. Soc.*, 2006, **128**, 15914–15920.
5 A. Sartorel, M. Carraro, A. Bagno, G. Scorrano and M. Bonchio, Asymmetric Tetraprotonation of γ-[(SiO_4)$W_{10}O_{32}$]$^{8-}$ Triggers a Catalytic Epoxidation Reaction: Perspectives in the Assignment of the Active Catalyst, *Angew. Chem., Int. Ed.*, 2007, **46**, 3255–3258.
6 K. Sugahara, S. Kuzuya, T. Hirano, K. Kamata and N. Mizuno, Reversible Deprotonation and Protonation Behaviors of a Tetra-Protonated γ-Keggin Silicodecatungstate, *Inorg. Chem.*, 2012, **51**, 7932–7939.
7 D. Patni and S. K. Jha, Protonation–Deprotonation Switch Controls the Amyloid-like Misfolding of Nucleic-Acid-Binding Domains of TDP-43, *J. Phys. Chem. B*, 2021, **125**, 8383–8394.
8 Q. Zhang, F. Xia, T. Sun, W. Song, T. Zhao, M. Liu and L. Jiang, Wettability switching between high hydrophilicity at low pH and high hydrophobicity at high pH on surface based on pH-responsive polymer, *Chem. Commun.*, 2008, **10**, 1199–1201.
9 J. Alves da Silva, J. Felcman, C. C. Lopes, R. S. C. Lopes and J. D. F. Villar, Study of the protonation/deprotonation sequence of two polyamines: bis-[(2S)-2-pyrrolidinylmethyl] ethylenediamine and spermidine by ^{1}H and ^{13}C nuclear magnetic resonance, *Spectrosc. Lett.*, 2002, **35**, 643–661.
10 S. K. Yamaguchi, K. Yonesato, S. Yamazoe, S. Kikkawa, D. Yokogawa, K. Yamaguchi and K. Suzuki, Variable control of the electronic states of a silver nanocluster via protonation/deprotonation of polyoxometalate ligands, *Chem. Sci.*, 2022, **13**, 5557–5561.

11 D. Zhang, H. Li, C. Li, Z. Wang, T. Li, N. Li, M. Cheng, J. Wang, J. Niu and T. Liu, A large molecular cluster with high proton release capacity, *Chem. Commun.*, 2020, **56**, 12849–12852.

12 L. Ruhlmann, L. Nadjo, J. Canny, R. Contant and R. Thouvenot, Di- and Tetranuclear Dawson-Derived Sandwich Complexes: Synthesis, Spectroscopic Characterization, and Electrochemical Behavior, *Eur. J. Inorg. Chem.*, 2002, **2002**, 975–986.

13 T. Minato, K. Suzuki, K. Kamata and N. Mizuno, Synthesis of α-Dawson-Type Silicotungstate $[\alpha\text{-}Si_2W_{18}O_{62}]^{8-}$ and Protonation and Deprotonation Inside the Aperture through Intramolecular Hydrogen Bonds, *Chem. – Eur. J.*, 2014, **20**, 5946–5952.

14 D. Zhang, Z. Liang, S. Xie, P. Ma, C. Zhang, J. Wang and J. Niu, A New Nb_{28} Cluster Based on Tungstophosphate, $[\{Nb_4O_6(OH)_4\}\{Nb_6P_2W_{12}O_{61}\}_4]^{36-}$, *Inorg. Chem.*, 2014, **53**, 9917–9922.

15 Z. Weng, Y. Ren, X. Li, B. Yue and H. He, Aggregation of Nb/W mixed addenda Dawson-type polyoxometalates units and lanthanide ions: Synthesis, characterization and electrocatalysis, *Polyhedron*, 2021, **195**, 114974.

16 Y. Wu, S. Morton, X. Kong, G. S. Nichol and Z. Zheng, Hydrolytic synthesis and structural characterization of lanthanide-acetylacetonato/hydroxo cluster complexes – A systematic study, *Dalton Trans.*, 2011, **40**, 1041–1046.

17 K. Y. Wang, B. S. Bassil, Z. Lin, I. Römer, S. Vanhaecht, T. N. Parac-Vogt, C. Sáenz De Pipaón, J. R. Galán-Mascarós, L. Fan, J. Cao and U. Kortz, Ln_{12}-Containing 60-Tungstogermanates: Synthesis, Structure, Luminescence, and Magnetic Studies, *Chem. – Eur. J.*, 2015, **21**, 18168–18176.

18 R. Copping, A. J. Gaunt, I. May, M. J. Sarsfield, D. Collison, M. Helliwell, I. S. Denniss and D. C. Apperley, Trivalent lanthanide lacunary phosphomolybdate complexes: a structural and spectroscopic study across the series $[Ln(PMo_{11}O_{39})_2]^{11-}$, *Dalton Trans.*, 2005, 1256–1262.